STATIC RESPONSE OF HOMOGENEOUS QUANTUM FLUIDS BY DIFFUSION MONTE CARLO

GAETANO SENATORE
INFM – Istituto Nazionale di Fisica della Materia, Dipartimento di Fisica Teorica, Università Trieste, strada Costiera 11, I-34014 Trieste, Italy

SAVERIO MORONI
INFM – Istituto Nazionale di Fisica della Materia, SISSA - Scuola Internazionale di Studi Avanzati, via Beirut 2-4, I-34014 Trieste, Italy

AND

DAVID M. CEPERLEY
NCSA – National center for Supercomputing Applications, Department of Physics, University of Illinois, Urbana, Illinois 61801

Abstract. We review the calculation of the static response of quantum fluids at $T = 0$ by diffusion Monte Carlo (DMC) simulations. In the first lecture we focus on the definition of response functions, routes to their computation, and practical details of the calculations. In the second lecture we survey specific results for the linear response of a number of simple fluids—^{4}He, the 3D electron gas, and the 2D electron gas—and we provide case by case some motivation as to why such a quantity should be of interest, commenting also on what we can learn from the results of simulations.

1. Zero temperature static response of a homogeneous fluid and ground state simulations

The concept of response[1, 2] naturally arises when the effect of a perturbation on a system is described in terms of deviations of the various properties (of the system) from their unperturbed values. In general one applies to the system a dynamical field, which couples to a specific observable and yet may

cause changes in all the properties of the system[3]. Here, we shall concentrate on static perturbations. We shall mention results pertaining to the general dynamical case when stating the fluctuation–dissipation (FD) theorem[4, 1, 2], which relates the static response to equilibrium fluctuations.

1.1. DENSITY–DENSITY STATIC RESPONSE

Let us consider a system of N interacting particles in a volume V, with Hamiltonian $\hat{H}_0$, at zero temperature. Ψ_0 is the ground state of such a system, with an energy E_0 and a one–body density $\rho_0(\mathbf{r})$. We apply to the system a *static* external potential $v(\mathbf{r})$ which couples to the one-body density operator $\hat{\rho}(\mathbf{r}) = \sum_{i=1}^{N} \delta(\mathbf{r} - \mathbf{r}_i)$ and ask what are the energy and density changes caused by such potential. We also mention, in passing, that a standard thermodynamic limit is implied ($N \to \infty$, $V \to \infty$, with $N/V = \rho_0$), both with and without external potential; moreover homogeneity and isotropy are assumed for the unperturbed system, implying $\rho_0(\mathbf{r}) = \rho_0$.

In the presence of the external potential, the Hamiltonian of the system becomes

$$\hat{H}_v = \hat{H}_0 + \int d\mathbf{r}\hat{\rho}(\mathbf{r})v(\mathbf{r}). \tag{1}$$

It is evident that the Hamiltonian $\hat{H}$ is a functional of $v(\mathbf{r})$ and therefore so are the ground state energy $E_v \equiv E_0[v]$ and the ground state density $\rho_v(\mathbf{r}) \equiv \rho_0(\mathbf{r}, [v])$. One can define the density-density response functions as the coefficients entering the functional expansion of $\rho_v(\mathbf{r})$ in terms of $v(\mathbf{r})$,

$$\begin{aligned} \delta\rho(\mathbf{r}) \quad &\equiv \quad \rho_v(\mathbf{r}) - \rho_0 = \\ &\sum_{k=1}^{\infty} \frac{1}{k!} \int d\mathbf{r}_1 \cdots d\mathbf{r}_k \chi^{(k)}(\mathbf{r}_1 - \mathbf{r}, \cdots, \mathbf{r}_k - \mathbf{r}) v(\mathbf{r}_1) \cdots v(\mathbf{r}_k). \end{aligned} \tag{2}$$

Here, $\chi^{(k)}(\mathbf{r}_1 - \mathbf{r}, \cdots, \mathbf{r}_k - \mathbf{r})$ is the density–density response function of order k, possessing all the obvious symmetries which follow from the assumed homogeneity and isotropy[1]. To obtain a similar expansion for the ground state energy first we note that the functional derivative of E_v with respect to $v(\mathbf{r})$ is the density,

$$\frac{\delta E_v}{\delta v(\mathbf{r})} = \rho_v(\mathbf{r}), \tag{3}$$

as it follows at once from first-order perturbation theory. Next we consider the identity

$$E_0[\lambda v] - E_0[0] = \int_0^{\lambda} d\lambda' \int d\mathbf{r} \rho_0(\mathbf{r}, [\lambda' v]) v(\mathbf{r}), \tag{4}$$

which can be easily demonstrated considering the ground state energy $E_0[\lambda v]$ as function of λ and exploiting Eq. (3). Using the explicit expression of $\rho_0(\mathbf{r},[\lambda' v])$ given in Eq. (2) in Eq. (4) and setting $\lambda = 1$, one readily obtains

$$\begin{aligned} E_v - E_0 &= \rho_0 \int d\mathbf{r} v(\mathbf{r}) + \sum_{k=1}^{\infty} \frac{1}{(k+1)!} \int d\mathbf{r} d\mathbf{r}_1 \cdots d\mathbf{r}_k \times \\ &\chi^{(k)}(\mathbf{r}_1 - \mathbf{r}, \cdots, \mathbf{r}_k - \mathbf{r}) v(\mathbf{r}) v(\mathbf{r}_1) \cdots v(\mathbf{r}_k). \end{aligned} \tag{5}$$

In terms of the Fourier components $v_{\mathbf{q}}$ of the external potential,

$$v(\mathbf{r}) = \sum_{\mathbf{q}} v_{\mathbf{q}} exp[i\mathbf{q} \cdot \mathbf{r}], \tag{6}$$

the density and energy changes become

$$\delta\rho(\mathbf{r}) = \sum_{k=1}^{\infty} \frac{1}{k!} \sum_{\mathbf{q}_1, \cdots, \mathbf{q}_k} \chi^{(k)}(\mathbf{q}_1, \cdots, \mathbf{q}_k) v_{\mathbf{q}_1} \cdots v_{\mathbf{q}_k} exp[i(\mathbf{q}_1 + \cdots + \mathbf{q}_k) \cdot \mathbf{r}], \tag{7}$$

and

$$\begin{aligned} \delta\varepsilon_v &\equiv \varepsilon_v - \varepsilon_0 = \frac{E_v}{N} - \frac{E_0}{N} = v_0 + \\ &\frac{1}{\rho_0} \sum_{k=1}^{\infty} \frac{1}{(k+1)!} \sum_{\mathbf{q}+\mathbf{q}_1+\cdots+\mathbf{q}_k=0} \chi^{(k)}(\mathbf{q}_1, \cdots, \mathbf{q}_k) v_{\mathbf{q}} v_{\mathbf{q}_1} \cdots v_{\mathbf{q}_k}, \end{aligned} \tag{8}$$

where we have introduced the energy change per particle ε and the Fourier transforms of the response functions with respect to their spatial arguments $\chi^{(k)}(\mathbf{q}_1, \cdots, \mathbf{q}_k)$.

Eqs. (7) and (8) give a series expansion of two particular ground state averages in powers of the set of coupling strengths $\{v_{\mathbf{q}}\}$, with the coefficients of the expansions being density–density response functions. Thus they provide practical routes to the estimate of static response, through the fitting of the calculated energy (or density) change to a function of the coupling strengths $\{v_{\mathbf{q}}\}$. Before discussing this point in detail we should mention an alternative route to the computation of the static response, which exploits the famous fluctuation–dissipation theorem[4, 1, 2] and only considers the unperturbed system, though dynamical properties need to be calculated.

1.2. STATIC RESPONSE AND EQUILIBRIUM FLUCTUATIONS

Above, we have considered the effect of a *static* perturbation on a given homogeneous system. A more general problem is the one in which one takes

a *dynamical* perturbation, which is *adiabaticly switched on* [1]. Restricting to the linear response and working in reciprocal space, it is fairly easy to show that the generalization of Eq. (7) reads

$$\rho_v(\mathbf{q},\omega) \quad = \quad \chi(q,\omega)v(\mathbf{q},\omega) + \cdots, \tag{9}$$

with $\rho_v(\mathbf{q},\omega)$ the Fourier transform of $\delta\rho(\mathbf{r},t)$ and $\chi(q,\omega)$ a complex function, $\chi(q,\omega) = \chi'(q,\omega) + i\chi''(q,\omega)$, which by virtue of causality satisfies Kramers–Kronig relations. These imply, in particular, a relation between the static response and the imaginary part of the dynamical response according to

$$\chi(q) = \chi(q,0) = \frac{2}{\pi}\int_0^\infty d\omega \frac{\chi''(q,\omega)}{\omega}. \tag{10}$$

The fluctuation dissipation theorem relates[1, 2] $\chi''(q,\omega)$, which describes the dissipation of energy in the system under the action of the perturbation, to the dynamical structure factor $S(q,\omega)$, which describes the equilibrium density fluctuations in the unperturbed system:

$$\chi''(q,\omega) = -\frac{\rho_0}{2\hbar}[S(q,\omega) - S(q,-\omega)] = -\frac{\rho_0}{2\hbar}[1 - e^{-\beta\hbar\omega}]S(q,\omega). \tag{11}$$

From Eqs. (10) and (11) and at $T = 0$ one immediately gets

$$\chi(q) = -\frac{\rho_0}{\pi\hbar}\int_0^\infty d\omega\, \frac{S(q,\omega)}{\omega}, \tag{12}$$

which expresses the static response in terms of $S(q,\omega)$. Finally, the dynamical structure factor

$$S(q,\omega) = \int_{-\infty}^{\infty} d\omega\, F(q,t)e^{i\omega t} \tag{13}$$

is just the Fourier transform of the intermediate scattering function

$$F(q,t) = \frac{1}{N}\langle\rho(\mathbf{q},t)\rho(-\mathbf{q},0)\rangle, \tag{14}$$

measuring time correlations between wavelike density fluctuations, in the unperturbed system. In cases in which the equilibrium average of Eq. (14) can be actually computed[5], one can readily obtain the static response exploiting Eqs. (12) and (13). This is the case for Bosons, say ^{4}He, both a finite[6] and at zero[7, 8] temperature, but it is still not feasible for Fermions. We therefore turn below to the discussion of ground state calculations for a (statically) perturbed fluid.

1.3. STATIC RESPONSE FROM GROUND–STATE CALCULATIONS FOR A PERTURBED FLUID

Above we have seen that calculations for a perturbed fluid contain information on response functions. Here we show how such information can be used to actually estimate response functions. It is evident that practical calculations are performed with small but finite external fields, implying the presence in Eqs. (7) and (8) of terms beyond the leading ones, involving in turn non–linear response functions. Such terms cannot be simply neglected and thus even restricting to the one–body density change one is faced with the fitting of a function depending on several variables (the set $\{v_{\mathbf{q}}\}$)—the fitting parameters being response functions.

Things simplify a lot if one considers a *monochromatic* external field

$$v(\mathbf{r}) = 2v_{\mathbf{q}} cos(\mathbf{q}\cdot\mathbf{r}) \tag{15}$$

Apart from having a single variable $v_{\mathbf{q}}$ ($\mathbf{q} \neq 0$) rather than a set, one also finds that in this case the energy change only contains even powers of the potential strength $v_{\mathbf{q}}$

$$\delta\varepsilon_v = \frac{\chi(q)}{\rho_0} v_{\mathbf{q}}^2 + \frac{\chi^{(3)}(\mathbf{q},\mathbf{q},-\mathbf{q})}{4\rho_0} v_{\mathbf{q}}^4 + \cdots. \tag{16}$$

Above we have dropped the superscript from the first-order (linear) response function. Similarly one finds that the density change with wavevector $\mathbf{q}$ is given by

$$\delta\rho(\mathbf{q};\mathbf{r}) = 2\rho_{\mathbf{q}} cos(\mathbf{q}\cdot\mathbf{r}), \tag{17}$$

with

$$\rho_{\mathbf{q}} = \chi(q) v_{\mathbf{q}} + \frac{\chi^{(3)}(\mathbf{q},\mathbf{q},-\mathbf{q})}{2} v_{\mathbf{q}}^3 + \cdots, \tag{18}$$

containing only odd powers of $v_{\mathbf{q}}$. It is clear that if one knows the energy (or density) change induced by a weak external potential, at few coupling strengths $v_{\mathbf{q}}$, Eq. (16) (or Eq. (18)) provides a straightforward, systematic route to the estimation of lower order response functions, by means of a suitable fit in powers of the potential strength $v_{\mathbf{q}}$. The problem of calculating response functions is thus changed into that of accurately evaluating properties of the many-body system in the presence of the perturbation of Eq. (15). This can be done by resorting to the Quantum Monte Carlo (QMC) method in its implementations for continuum systems[9, 10, 11].

1.4. DIFFUSION MONTE CARLO AND TRIAL WAVEFUNCTION

Of the various simulation techniques which go under the name of QMC, one in particular has been extensively used to estimate the density–density linear response in quantum fluids[12, 13, 14, 15, 16, 17, 18, 19]: the Diffusion Monte Carlo (DMC) method[10, 20, 11]. As this technique is reviewed elsewhere[21] in this book, to avoid unnecessary duplication here we shall skip all the details of the method ad concentrate on its application.

We just mention—also to fix the notation—that in DMC one propagates in imaginary time the N–particle wavefunction $\Phi(R,\tau)$, starting from a suitable initial condition$\Phi(R,\tau=0)$. Usually one takes $\Phi(R,\tau=0)=\Psi(R)$, with $\Psi(R)$ a trial wavefunction which already provides an accurate description of the system under consideration. Here, $R\equiv(\mathbf{r}_1,\mathbf{r}_2,\ldots,\mathbf{r}_N)$ is the set of coordinates of the many–body system. The imaginary time evolution projects out the lowest energy component of $\Psi(R)$, as is seen by expanding the initial condition in exact eigenstates of the hamiltonian,

$$\Phi(R,0)=\Psi(R)=\sum_{n=0}^{\infty}c_n\Psi_n(R), \tag{19}$$

yielding

$$\Psi(R,\tau)=\sum_{n=0}^{\infty}c_n e^{-(E_n-E_T)\tau}\Psi_n(R)\to c_0 e^{-(E_0-E_T)\tau}\Psi_0(R),\quad \tau\to\infty. \tag{20}$$

In practice, for reasons of efficiency one propagates the mixed distribution $f(R,\tau)=\Phi(R,\tau)\Psi(R)$, which for large times goes into $f(R)\propto\Psi_0(R)\Psi(R)$. Working with $f(R,\tau)$ also allows to conveniently apply the wavefunction antisymmetry when dealing with Fermions, by assuming that the nodes of $\Psi_0(R)$ coincide with those of $\Psi(R)$—an approximation that is know as fixed–node[10]. In the following, for Fermions we shall always restrict to such an approximation. Evidently the capability of sampling $\Psi_0(R)\Psi(R)$ allows the estimate of ground state properties.

We should mention at this point that as far as the estimate of linear response is concerned Eqs. (16) and (18) are equivalent—if one is able to sample energy and density changes with comparable accuracy. In principle one might prefer the density route, on the ground that for small external fields the density change should be larger. In fact, density and energy changes scale respectively linearly and quadratically with $v_{\mathbf{q}}$, to leading order. In practice the situation may be reversed. In DMC energy estimates are exact for the given nodes and within statistical errors, whereas other averages such as the one–body density involve a systematic error[22] which scales with $(\Psi-\Psi_0)^2$—if obtained as extrapolated estimates[21, 9]. Though

we did perform few calculations using extrapolated estimates of Eq. (18)—as a test of internal consistency of our simulations, we generally evaluated $\chi(q)$ using the energy route of Eq. (16)[23].

The choice of the trial wavefunction $\Psi(R)$ is an important step in all DMC simulations, in that $\Psi(R)$ determines the efficiency of the propagation process. For Fermions the choice of $\Psi(R)$ is in fact crucial as it fixes (approximates) the nodes of the sought ground state and thus determines the accuracy of the ground state energy, and more in general of all the ground state averages. We shall illustrate this point in detail below. Before doing so, we have to discuss the explicit form of the trial wavefunctions that we have used in our DMC simulations for Bosons[12] and for Fermions[12, 16].

1.4.1. *Trial wavefunction for Bosons*
A simple choice for Ψ, to study the uniform superfluid phase of ^{4}He, is to take as in earlier simulations[24] on this system a Jastrow trial function

$$\Psi^0 = J^0 = \prod_{i<j} exp[-u(r_{ij})], \tag{21}$$

with $u(r)$ a pair pseudopotential of the McMillan form. By sticking to the energy route, we have no need[12] in DMC to go to more sophisticated wavefunctions[25], which are instead crucial for variational Monte Carlo (VMC) simulations.

Similarly, for the perturbed fluid a reasonable choice is

$$\Psi^v(\alpha) = \Psi^0 \prod_i exp[\alpha\, cos(\mathbf{q}\cdot\mathbf{r}_i)], \tag{22}$$

with α a variational parameter which is fixed minimizing the expectation value

$$E(\alpha; v_{\mathbf{q}}) = \langle \Psi^v(\alpha) | \hat{H}_{\mathbf{q}} | \Psi^v(\alpha) \rangle \tag{23}$$

of the perturbed Hamiltonian

$$\hat{H}_{\mathbf{q}} = \hat{H}_0 + \sum 2\, v_{\mathbf{q}} cos(\mathbf{q}\cdot\mathbf{r}_i). \tag{24}$$

Note that, to leading order in α, $\Psi^v(\alpha)$ yields a density

$$\rho(\mathbf{r}) = \rho_0 + 2\alpha(v_{\mathbf{q}})\gamma(\rho_0) cos(\mathbf{q}\cdot\mathbf{r}), \tag{25}$$

which is precisely of the form given in Eq. (17). In fact if one uses only energy estimates, strictly there is no need to struggle and optimize the trial function Ψ, as converged DMC estimates of the ground state energy of a Bosonic system are independent of Ψ, provided this is symmetric.

1.4.2. *Trial wavefunction for Fermions*
For Fermions one usually factorizes the trial function in two pieces: a symmetric term roughly accounting for correlations and an antisymmetric term which, as far as DMC is concerned, fixes the nodes of the wavefunction. In the literature on electrons in 3[26, 27, 28] and in 2[29] dimensions the simplest trial function for the uniform fluid phase is

$$\Psi^0 = D_\uparrow D_\downarrow J^0. \tag{26}$$

The correlation term $J^0 = \prod_{i<j} exp[-u(r_{ij})]$ is taken again of the Jastrow type, as for Bosons (see, Eq. (21)), with $u(r)$ an RPA pseudopotential[26]. The antisymmetric term fixing the nodes, on the other hand, is a product of plane–wave Slater determinants, D_σ denoting the determinant for the N_σ particles with spin projection σ. Note that the wavefunction written in Eq. (26) in general is not fully antisymmetric, as it gives just one spin component of the full trial function. However, exploiting particle identity it is easily shown that averages on the Ψ^0 of Eq. (26) coincide with averages on the full trial function[30]. The same applies to DMC averages obtained starting from such trial function.

For the perturbed fluid an obvious generalization of Eq. (26) is to take

$$\Psi^v(\alpha) = D^v_\uparrow D^v_\downarrow J^0, \tag{27}$$

where D^v_σ is a Slater determinant of one–particle orbitals in an external field

$$v(\mathbf{r}) = 2\,\alpha\, cos(\mathbf{q}\cdot\mathbf{r}), \tag{28}$$

with an effective strength α. Note that as the one–particle orbitals (Mathieu functions) entering D^v_σ depend on α so does the nodal surface of $\Psi^v(\alpha)$. Evidently, the effective field strength is determined minimizing the expectation value of of $\hat{H}_\mathbf{q}$ on Ψ^v, which gives back Eq. (23). Thus, $\alpha = \alpha(v_\mathbf{q})$ and the nodal surface of Ψ^v finally depends on $v_\mathbf{q}$.

The choice of Eq. (27) is sort of obvious in the sense that one takes for the modulated system the exact nodes of independent particles, as modified by the presence of a monochromatic potential (Eq. (28)). Such potential, however, though being of the same periodicity as the the external potential of Eq. (15), has a different optimal strength. Note that, due to the minimization alluded above, α depends in general also on the pseudopotential $u(r)$ appearing in the Jastrow term—which we keep identical to the one used in the uniform liquid and therefore independent of both $\mathbf{q}$ and $v_\mathbf{q}$. For the Fermi liquid a trial function of the form given in Eq. (22), with Ψ^0 from Eq. (26) is of no particular interest, as it would have the same nodes as Ψ_0,

whereas the choice made above gives an explicit parameterization of the nodal surface of Ψ^v in term of α.

We should mention here that in our response calculations we made no attempt to use more sophisticated nodes, as those explored in detail for the uniform electron gas[29, 28]. A partial justification of this makes appeal to the fact that changing the nodes in both the uniform and modulated Fermi fluid is likely to give a small effect in the response, if this is calculated from the energy difference between the two phase, because of cancellation. In other words, what matters is the precision with which one calculates the energy differences and not the precision of the energy of the individual phases. We shall explicitly illustrate this point later on, with regard to the time step error present in DMC.

1.5. OPTIMIZATION OF THE TRIAL WAVEFUNCTION

Both for Bosons and Fermions the optimization of the trial wavefunction involves the minimization of the expectation value of the energy on the trial wavefunction

$$\begin{aligned} E(\alpha; v_{\mathbf{q}}) &= E_{int}(\alpha) + \int d\mathbf{r}\, \rho(\mathbf{r};\alpha)\, v(\mathbf{r}) \\ &= E_{int}(\alpha) + 2\rho(\mathbf{q};\alpha)\, v_{\mathbf{q}}. \end{aligned} \tag{29}$$

Above, the internal energy E_{int} is given by

$$E_{int}(\alpha) = \langle \Psi^v(\alpha) | \hat{H}_0 | \Psi^v(\alpha) \rangle, \tag{30}$$

and, clearly,

$$\rho(\mathbf{r};\alpha) = \langle \Psi^v(\alpha) | \hat{\rho}(\mathbf{r}) | \Psi^v(\alpha) \rangle. \tag{31}$$

The minimization of $E(\alpha; v_{\mathbf{q}})$ with respect to $v_{\mathbf{q}}$ involves solving the extremum condition

$$\frac{dE_{int}(\alpha)}{d\alpha} + 2v_{\mathbf{q}} \frac{d\rho(\mathbf{q};\alpha)}{d\alpha} = 0. \tag{32}$$

The above equation can be solved either for α, finding the optimal effective potential corresponding to a given $v_{\mathbf{q}}$, or for $v_{\mathbf{q}}$ to find the external field for which a given α is optimal. While the two routes are in principle equivalent and choosing one or the other corresponds to determine the function $\alpha(v_{\mathbf{q}})$ or its inverse $v_{\mathbf{q}}(\alpha)$, in practice the second route is much more convenient as it has an explicit solution

$$v_{\mathbf{q}} = -\frac{dE_{int}(\alpha)}{d\alpha} \Big/ \left(2\frac{d\rho(\mathbf{q};\alpha)}{d\alpha} \right), \tag{33}$$

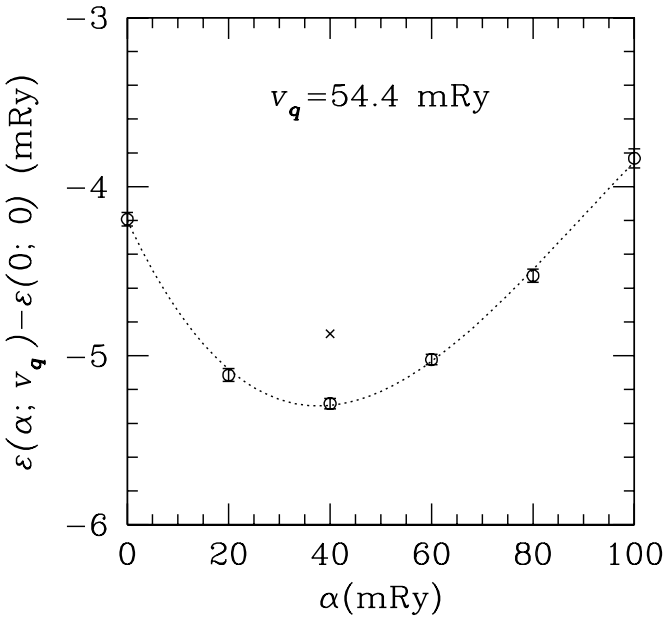

Figure 1. Dispersion of the DMC energy versus the effective field strength α, providing a partial parameterization of the wavefunction nodal surface. The circles (with error bars) give the computed DMC fixed–node energies, whereas the cross gives the VMC energy at the optimal effective strength. The line is a fit to the DMC points. The data shown are for the unpolarized electron gas in 2 dimensions at $r_s = 2$, placed in a monochromatic external field of strength $v_{\mathbf{q}}$ with $q = 1.9q_F$; $N = 42$. The density parameter r_s is defined by $\pi r_s^2 a_0^2 = 1/\rho_0$, with a_0 the Bohr radius, and $q_F = \sqrt{2}/r_s a_0$ is the Fermi wavevector.

in terms of derivatives of the internal energy and the one body density with respect to α. In fact, using the re–weighting technique[31, 30], $dE_{int}(\alpha)/d\alpha$ and $d\rho(\mathbf{q};\alpha)/d\alpha$ can be efficiently computed for a given α from a single set of configurations sampled from the probability density $|\Psi^v(\alpha)|^2$. This bypasses the problem of statistical noise that would otherwise affect the finite difference evaluation of derivatives, if one used different sets of configurations for slightly different values of α.

We have noted above that in total energy calculations the optimization of the trial wavefunction is not that important for Bosons. Accordingly, below we shall restrict our discussion on the optimization of Ψ^v to Fermions, for which the optimizion of nodes has proven crucial in obtaining accurate results[16]

1.5.1. *Optimization of the nodal structure for the nonuniform Fermion fluid*

As we have mentioned above, the optimization of the trial functionΨ^v proceeds by determining the external field strength $v_{\mathbf{q}}$ which corresponds to a fixed small value of the variational parameter α^* by computing Eq. (33) via a MC sampling. This procedure determines, within our simple parameterization, the VMC optimal optimal nodes, which we then use in our DMC simulations in the fixed–node approximation. A priori it is not obvious how good are these nodes for the DMC simulations. This, however, can be checked very simply by performing DMC simulations with deoptimized wavefunctions, i.e., with $\alpha \neq \alpha*$, for the given $v_{\mathbf{q}}$. In the few cases we have checked it turns out that the the VMC optimal nodes are in fact nearly optimal also for DMC, as it is clearly illustrated in Fig. 1, for the 2 dimensional electron gas.

For the particular case examined in Fig. 1 the optimal effective field strength α is about 26% smaller than the external strength $v_{\mathbf{q}}$. One may ask whether the ratio $v_{\mathbf{q}}/\alpha$ has any regularity, namely whether it depends appreciably on q and whether it depends on the perturbation that one is considering. The answer to this question is given in Fig. 2 where $v_{\mathbf{q}}/\alpha$ is shown as a function of q, again for for the 2 dimensional electron gas at various densities. First of all we find that $v_{\mathbf{q}}/\alpha$ may substantially deviate from 1, reaching values as large as 4 and as small as 0.2. Second, at small wavevectors effective and external fields sensibly deviate from the each other, but they tend to become equal for large wavevectors. This does not come as a surprise, as one would expect the effect of the interparticle interactions to become minor at large wavevectors. Third, at small wavevectors the effect of interparticle interactions is different on charge and spin perturbations, bringing about effective fields which are respectively weaker and stronger that the externally applied field. If one assumes that the effective field α roughly coincides with the Kohn–Sham effective potential v^{KS}[32] of density functional formalism[33, 32, 34], this behavior can be easily understood by linearizing v^{KS} with respect to the external field[35]. We remind the reader that $v^{KS}(\mathbf{r})$ is that particular external one–body potential which produces in a system of non–interacting particles the same one–body density $\rho(\mathbf{r})$ of the interacting system placed in the actual external potential.

1.6. TYPICAL OUTPUT OF A LINEAR RESPONSE CALCULATION

Evidently, wavefunction optimization is an important but preliminary part of response function calculations, in the scheme outlined above. The central part of the calculation, remains the DMC estimate of ground state averages

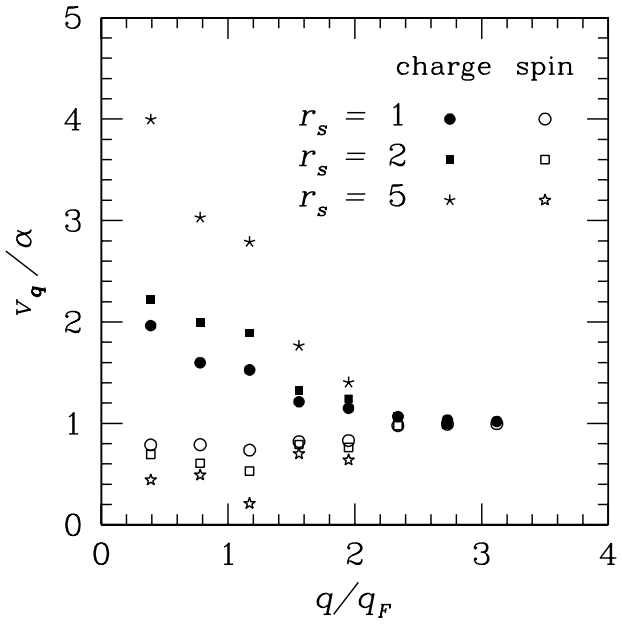

Figure 2. Deviation of the optimal effective field strength α from the the external field strength $v_{\mathbf{q}}$, as function of the wavevector q. Results for the 2 dimensional electron gas at various densities and $N = 42$ are shown for two different perturbations, coupling one to the charge density and the other to the spin density.

as a function of a (weak) external coupling. Once such dispersion curves have been obtained, a simple fitting procedure allows one to estimate the sought response functions. Here we give two detailed examples of the results of DMC calculations of the spin response for the 2 dimensional unpolarized electron gas at $r_s = 5$ (see the caption to Fig. 1 for the definition of r_s). We should caution the reader that there are minor changes in the definition of spin response, compared with the definition of charge response given above, and they are reviewed in in Sec. 2.2.4.

In Fig. 3 we show the energy dispersion as function of the external field strength $h_{\mathbf{q}}$, together with its fitting function which reproduces the calculated DMC points with very good accuracy. Note that a quartic term is present in the fit and, though the error on the coefficient of such term is sizeable, still the term cannot be neglected. We caution the reader that the data shown are for a finite number of particles and in order to obtain results in the thermodynamic limit a size correction has to be applied to the numbers shown in the figure. This important point will be briefly touched

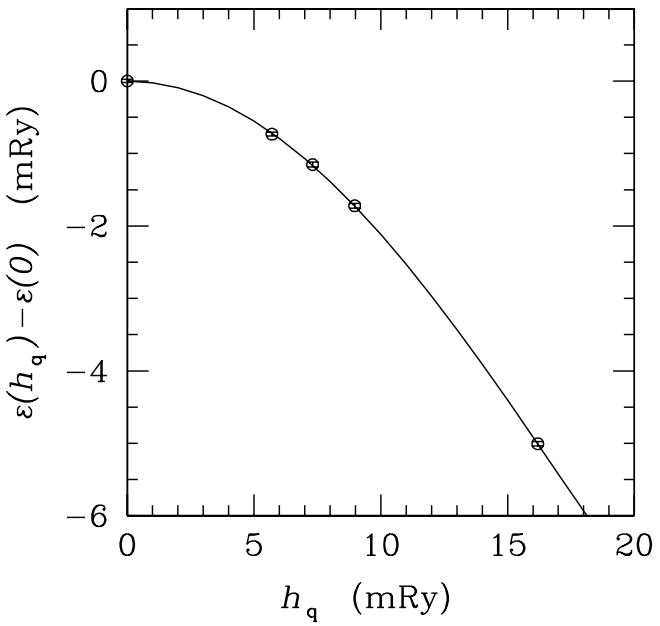

Figure 3. Calculated DMC energy (circles, with error bars) for a 2 dimensional unpolarized electron gas at $r_s = 5$ and $q = 1.9q_F$, as function of the applied magnetic field strength $H_{\mathbf{q}}$. Here $h_{\mathbf{q}} = (\mu_B g/2)H_{\mathbf{q}}$ [see Sec. 2.2.4 for the notation] and $N = 42$. The line is a quartic fit $\alpha + \beta h_{\mathbf{q}}^2 + \gamma h_{\mathbf{q}}^4$ to the calculated points, with $\alpha = -0.299764(19)$Ry, $\beta = -22.45(59)\text{Ry}^{-1}$, $\gamma = 12789(2136)\text{Ry}^{-3}$, and a reduced $\chi^2 = 0.20$.

later below.

In Fig. 4 we give the dispersion of the magnetization as function of the applied external magnetic field. Again, the DMC estimates are well reproduced by the fit, which in fact from the uncertainties on the parameters looks slightly more accurate than the one for the energy. However, one should regard the parameters obtained from the energy route as more reliable—since the values of $m_{\mathbf{q}}$ are extrapolated estimates and thus affected by an error which cannot be quantified systematically. Such extrapolation error justifies also the difference between the energy and magnetization estimates of β (essentially the linear spin response), which are well beyond the combined error bars[36]. Whereas the error on the energy estimate of β is reasonably small, the one on the estimate of γ—which is a cubic response function—allows one to establish only the order of magnitude of such a quantity.

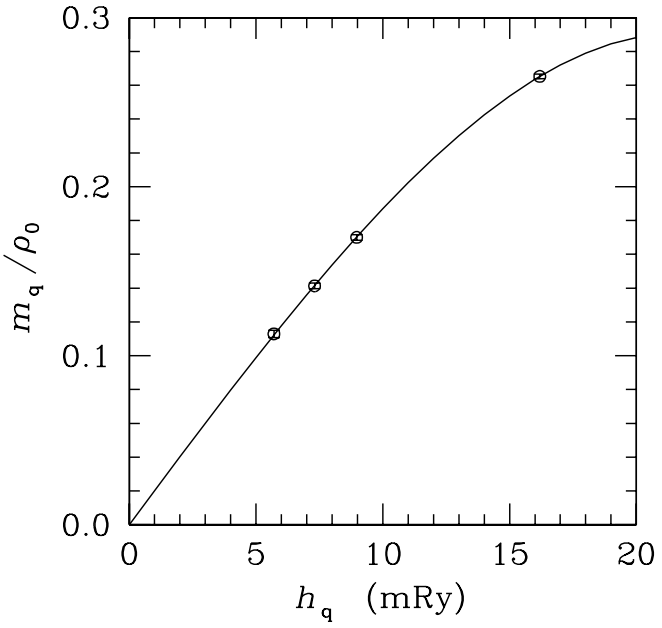

Figure 4. Calculated magnetization (circle, with error bars) for the same system as in Fig. 3. Here the magnetization density $m_{\mathbf{q}}$ is measured in units of $\mu_B g/2$ and the reduced magnetic field is defined as $h_{\mathbf{q}} = (\mu_B g/2)H_{\mathbf{q}}$. The line is a cubic fit $\beta h_{\mathbf{q}} + 2\gamma h_{\mathbf{q}}^3$ to the calculated points, with $\beta = 20.13(18)\mathrm{Ry}^{-1}$, $\gamma = -7146(401)\mathrm{Ry}^{-3}$, and a reduced $\chi^2 = 0.07$.

1.7. CORRECTING FOR SYSTEMATIC ERRORS: TIME STEP AND NUMBER EXTRAPOLATIONS.

DMC simulations require the sampling of the imaginary time propagator $G(R, \tau)$[9, 10, 21], which is not know in closed form. The short time approximations which are used to construct $G(R, \Delta\tau)$[9, 10, 21] involve a systematic error that vanishes with $\Delta\tau$ and should be extrapolated out. Similarly, actual simulations are performed for a finite number of particles and this introduces an additional bias that should be eliminated—if one wants to make prediction for an infinite system. Here, we briefly touch these to points, specializing to the calculation of response.

1.7.1. *Time step error*

We have already mentioned above that, to obtain acceptable accuracy for energy differences, one may often need to push calculations less than for the individual energies. This is precisely the case for time step extrapola-

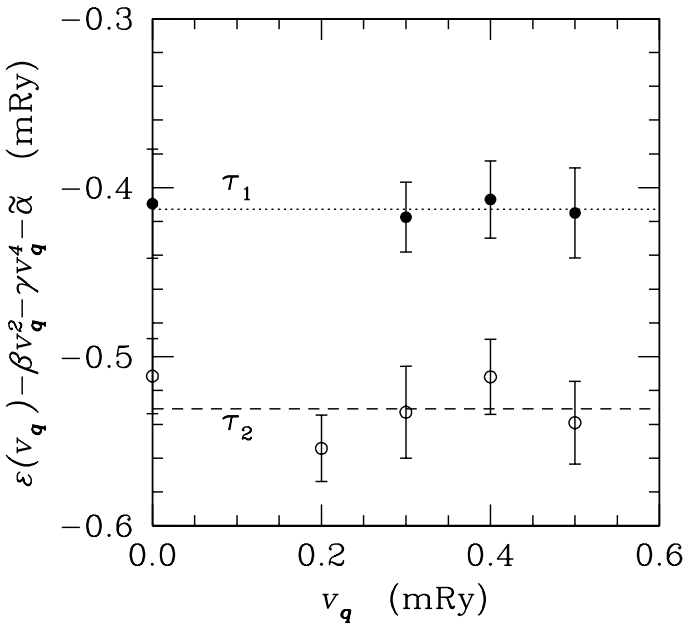

Figure 5. Fit of the calculated DMC ground state energy per particle, for two different time steps $\Delta\tau = \tau_1, \tau_2$. For clarity the non constant part of the the fitting function $\alpha + \beta v_{\mathbf{q}}^2 + \gamma v_{\mathbf{q}}^4$ and the common constant $\tilde{\alpha} = -303$mRy have been subtracted from $\varepsilon(v_{\mathbf{q}})$. Shown is the case of the 2 dimensional unpolarized electron gas at $r_s = 5$, $q = 4.7 q_F$ and $N = 18$. For $\tau_1 = 0.150\text{Ry}^{-1}$ we get $\beta_1 = -0.3026(5)\text{Ry}^{-1}$and a reduced $\chi^2 = 0.1$; for $\tau_2 = \tau_1/2$ we get $\beta_2 = -0.3024(5)\text{Ry}^{-1}$ and $\chi^2 = 1.5$. The dashed and dotted line give α_1 and α_2, respectively.

tion. In principle, the elimination of the time step error involves performing simulations with different (small) values of $\Delta\tau$ to then extrapolate each ground state estimate to $\Delta\tau = 0$. In practice, in our investigation on the response, we have performed simulations with a couple of suitably small time steps in selected cases and checked that the estimated response would be the same for the two different values of $\Delta\tau$. In Fig. 5 we illustrate this procedure for a density response calculation of the 2 dimensional electron gas, showing the DMC energy dispersion for two different values of $\Delta\tau$. It is evident that halving the time step does not change the estimate of the the linear density–density response function, though the individual energies are rigidly shifted by a tenth of mRy, beyond the combined error bars. Thus one can consider the response calculation converged with respect to the systematic time step error even though the individual energies are not.

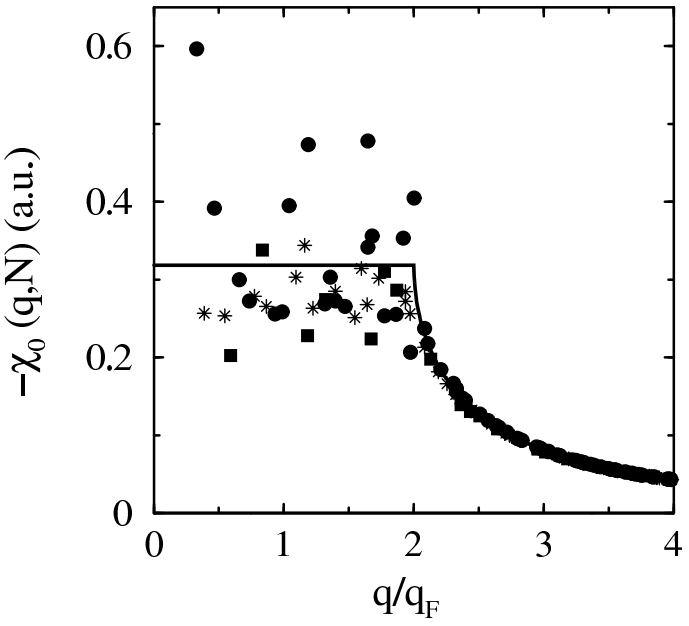

Figure 6. Number dependence of the density–density response of a non–interacting unpolarized Fermion system in 2 dimensions. The Stern function [37] is shown for $N = 18$ (squares), $N = 42$, (stars), $N = 58$ (circles), and in the thermodynamic limit (solid line)

1.7.2. *Size effects and number extrapolation*

Size effects enter actual simulations directly through the finite number of particles N and indirectly through the boundary conditions. Thus with the commonly used periodic boundary conditions only q's which are reciprocal lattice vectors of the simulation box are allowed. If studying a $\mathbf{q}$ independent quantity, like the ground state energy, the manner to correct for the finite value of N is simple. One studies $\varepsilon(N)$ as function of $1/N$ and extrapolates to $1/N = 0$ using more or less educated guesses[26] for the functional form of the fit. Unfortunately, when turning to functions of $\mathbf{q}$ and for Fermi liquids—to which we restrict the following discussion—one is faced with the fact that for given average density the sets of allowed wavevectors are generally different for different N, as illustrated in Fig. 6. Thus a systematic extrapolation as for the energy is out of question.

Some insight may be gained by looking at the behavior of a system of non–interacting particle. Thus in Fig. 6 we show the response function $\chi_0(\mathbf{q}; N)$ of a 2 dimensional unpolarized non–interacting Fermi liquid, for three different finite values of N and in the thermodynamic limit. Note that the chosen values of N are representative of those actually used in

simulation of the 2 dimensional electron gas, corresponding to closed shell configurations in the space of reciprocal lattice vectors. The size dependence of $\chi_0(\mathbf{q};N)$ is quite substantial, as is clearly appreciated from the figure, and in fact one can show that it does not display any sign of saturation even at N of few hundreds, which is already prohibitively large. A similar situation is found when turning to charged Fermi liquids[12, 16]. Thus, for these systems, one is in the very unpleasant situation of having a sizeable, in fact dramatic, N dependence and yet no simple *unbiased* recipe to perform a $1/N$ extrapolation.

Guided by the observation that both interacting and non–interacting responses have similar size dependence, one can try to exploit the exact knowledge of $\chi_0(\mathbf{q};N)$. (Remember that in extrapolating the ground state energy to $1/N=0$ one exploits what is known on the non–interacting ground state energy[26].) A simple guess could be to assume that $\chi(\mathbf{q};N)-\chi_0(\mathbf{q};N)$ has negligible dependence on N. A variant, which has been actually used[15], is to assume that this holds for $\chi(\mathbf{q};N)-\chi_{RPA}(\mathbf{q};N)$, with $\chi_{RPA}(\mathbf{q};N)$ the Random Phase Approximation (RPA) response function[38]. In fact, one can come up yet with another recipe[16] working with the inverse of the response and focusing on the quantity

$$v_c(q)G(\mathbf{q};N)=\frac{1}{\chi(\mathbf{q};N)}-\frac{1}{\chi_{RPA}(\mathbf{q};N)}=\frac{1}{\chi(\mathbf{q};N)}-\frac{1}{\chi_0(\mathbf{q};N)}+v_c(q) \quad (34)$$

with $v_c(q)$ the Coulomb coupling ($v_c(q)=4\pi e^2/q^2$, and $2\pi e^2/q$, respectively in 3 and in 2 dimensions). The ansatz in this case is

$$G(\mathbf{q})\equiv G(\mathbf{q};\infty)\approx G(\mathbf{q};N), \quad (35)$$

which states that finite size errors on the so called local field factor[39] of the electron gas are negligible, in accord with the notion that $G(\mathbf{q})$ describes exchange and correlation effects, which should be short ranged (see, e.g., Secs. 2.2.1 and 2.2.4). To date this last scheme for number extrapolation has proven to be the best[16], as we shall briefly illustrate in the next section.

2. Zero temperature static response of selected quantum fluids

The computational scheme that we have exposed above in some detail has been applied, in the last few years, to calculate of the linear density–density static response of model quantum liquids, such as ^{4} He[12], the 2 and 3 dimensional electron gas[12, 15, 16], the charged Bose fluid[13]. Recently, we have also computed the linear spin response[40] of the unpolarized 2 dimensional electron gas and we are now estimating the same quantity for the 3 dimensional electron gas. Below we shall briefly illustrate some of these applications. In all cases, before summarizing the DMC results, we

shall give the non–interacting response and mention some of the simplest theoretical approximations.

2.1. SUPERFLUID ^{4}HE

Helium remains fluid down to zero temperature, under vapor pressure, displaying striking quantum effects such as superfluidity, in both its natural isotopes—the Bose ^{4}He and the Fermi ^{3}He. For this reason it is one of the most studied quantum liquids[38] and ^{4}He, which becomes superfluid below $2.17K$, is the only quantum fluid for which the static density–density response function has been experimentally obtained[41]. In fact, the dynamical structure factor $S(q,\omega)$ was measured over a large range of frequencies at a temperature of $1.1K$ and $\chi(q)$ was calculated from Eq. (12).

The existence of experimental data makes the study of ^{4}He a natural test case. Moreover, being ^{4}He a Bose fluid, the DMC method provides an essentially exact calculation scheme, once a choice is made[12] for the interparticle interaction[42]. Before comparing our zero temperature results for $\chi(q)$ with the experimental evidence, we shall remind the reader of a few simple facts. The linear density–density response of a non–interacting Bose system is

$$\chi_0(q) = -\frac{4m\rho_0}{\hbar^2 q^2}. \tag{36}$$

Also, one of the simplest approximations to $\chi(q)$ in this context is the so–called Feynman approximation[43]

$$\chi_F(q) = -S(q)^2\,\frac{4m\rho_0}{\hbar^2 q^2}, \tag{37}$$

which relates $\chi(q)$ to the square of the static structure factor

$$S(q) = \int_{-\infty}^{\infty} \frac{d\omega}{2\pi} S(q,\omega). \tag{38}$$

It may be noted that, in the Feynman approximation, the monotonous $\chi_0(q)$ is modulated by the square of $S(q)$—which displays a peak and some oscillations in a strongly correlated fluid, such as ^{4}He, as it can be checked elsewhere[7] in this book.

In Fig. 7 we compare the DMC result for $\chi(q)$ with the experimental estimate of the same quantity and with the Feynman approximation. It is evident that the DMC points compare favorably with experiments, whereas the Feynman approximation performs rather poorly—especially in the peak region. In particular the Feynman approximation underestimates the structure found in the true response, for which it is an exact upper bound[43]

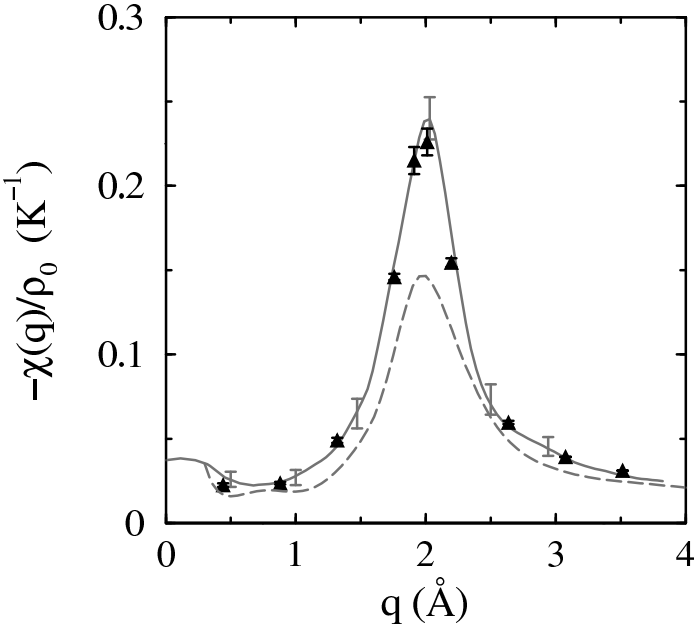

Figure 7. Density–density static response function $\chi(q)$ of superfluid ^{4}He at zero temperature and density $\rho_0 = 0.02186\mathring{A}^{-3}$. The triangles (with error bars) give the DMC result, obtained with $N = 64$, while the full curve is the experimental evidence [41], at small but finite temperature, $T = 1.1K$. Typical error bars are also shown for the experiment. The dashed curve gives the Feynman approximation (see text).

($\chi_F(q) \geq \chi(q)$). The non–interacting response has not been shown, since it does not bear any relation with the behavior found in the interacting system, apart from the large q region, where the effect of interactions becomes negligible. We mention here that for a neutral Bose system, such as ^{4}He, the size effects on the calculated response are essentially negligible, as we checked in a few test cases, performing simulations both with 64 and 125 particles. Our results should be compared with those recently obtained with the reptation QMC[7].

2.2. THE ELECTRON GAS

The electron gas[39, 44]—a model system of electrons moving in a uniform neutralizing charge background—is one the of the simplest yet most studied many–body models. It is not only a toy for theorists, its properties being more or less directly related to those of physical systems, both in 2[39, 45,

44] and 3 dimensions[39, 46]. Let us briefly recall here few notions about the density (or dielectric) response in the electron gas, before discussing our DMC results on the linear response.

2.2.1. *Non–interacting and approximate response; the local field*
For conciseness here we collect some results for both the 2 and 3 dimensional electron gas. We denote the Fourier transform of the pair interaction e^2/r by $v_c(q)$, with

$$v_c(q) = \frac{2(d-1)\pi e^2}{q^{d-1}}, \tag{39}$$

and d the spatial dimension, $d = 2, 3$.

It is straightforward to calculate the response of the non–interacting electron gas. One obtains in 2d the Stern function[37]

$$\chi_0(q) = -g\frac{m}{2\pi\hbar^2}\left[1 - \theta(q-2q_F)\sqrt{1-\left(\frac{2q_F}{q}\right)^2}\right], \tag{40}$$

and in 3d the Lindhard function[39]

$$\chi_0(q) = -g\frac{mq_F}{2\pi^2\hbar^2}\left[1 + \frac{q_F}{q}\left(1-\left(\frac{q}{2q_F}\right)^2\right)\ln\left|\frac{q+2q_F}{q-2q_F}\right|\right]. \tag{41}$$

The Stern function, is shown in Fig. 6. Above, $g = 1, 2$ is the degeneracy factor, respectively for the polarized and unpolarized Fermi system.

For the interacting case, the simple mean field argument that the response to the Hartree field (which is the sum of the external and the charge polarization fields) is approximately given by $\chi_0(q)$, yields at once[39] the famous RPA approximation[38, 39],

$$\chi_{RPA}(q) = \frac{\chi_0(q)}{1 - v_c(q)\chi_0(q)}. \tag{42}$$

Evidently the above argument is missing exchange and correlation effects and these can be conveniently measured by the difference between the full and RPA inverse responses,

$$v_c(q)G(q) = \frac{1}{\chi(q)} - \frac{1}{\chi_{RPA}(q)} = \frac{1}{\chi(q)} - \frac{1}{\chi_0(q)} + v_c(q), \tag{43}$$

defining a *local field factor* (or function) $G(q)$[38, 39]. In terms of $G(q)$ the exact response takes a generalized RPA form

$$\chi(q) = \frac{\chi_0(q)}{1 - v_c(q)[1-G(q)]\chi_0(q)}, \tag{44}$$

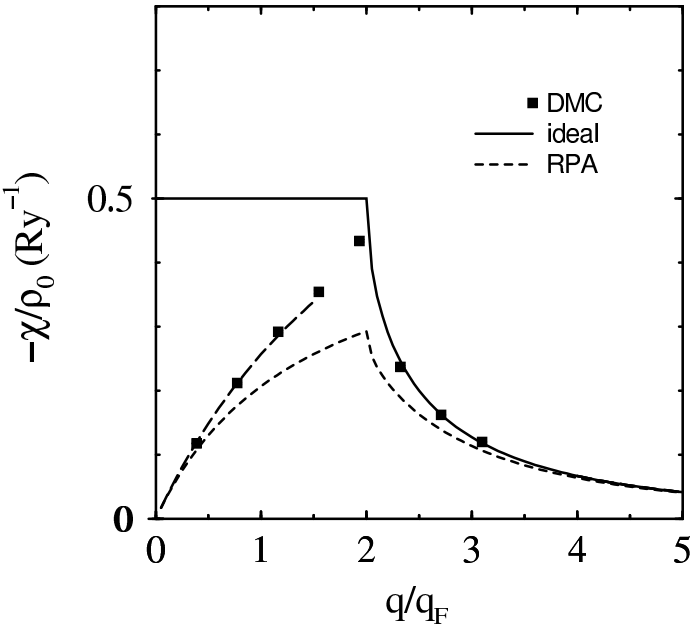

Figure 8. Density–density static response function $\chi(q)$ of the 2d electron gas at $r_s = 1$. The squares give the DMC prediction with error bars. The non–interacting (ideal) and RPA responses are respectively given by the full and the short-dashed curve, whereas the exact[14] small q behavior is shown by the long-dashed curve. The exact large q behavior is not distinguishable from the ideal response for $q > 4q_F$.

with the bare coupling $v_c(q)$ replaced by an *effective* coupling $v_c(q)[1-G(q)]$. This is reminiscent of the Clausius–Mossotti treatment of local fields in a dielectric[46]. The local field factor, which describes the exchange and correlation effects in the response, offers also a convenient way to specify approximate schemes beyond RPA, two of the most common being the Hubbard[38, 39] and the STLS[39] approximations. We refer the interested reader to Ref. [39] for a comprehensive compilation of approximations as of 1981. Moreover the local field function is related to the density functional theory (DFT)[33, 32], via the relations[47]

$$f_{xc}(q) = -v_c(q)G(q), \tag{45}$$

and

$$f_{xc}(|\mathbf{r}-\mathbf{r}'|) = \left[\frac{\delta^2 E_{xc}[\rho]}{\delta\rho(\mathbf{r})\delta\rho(\mathbf{r}')}\right]_{\rho_0}, \tag{46}$$

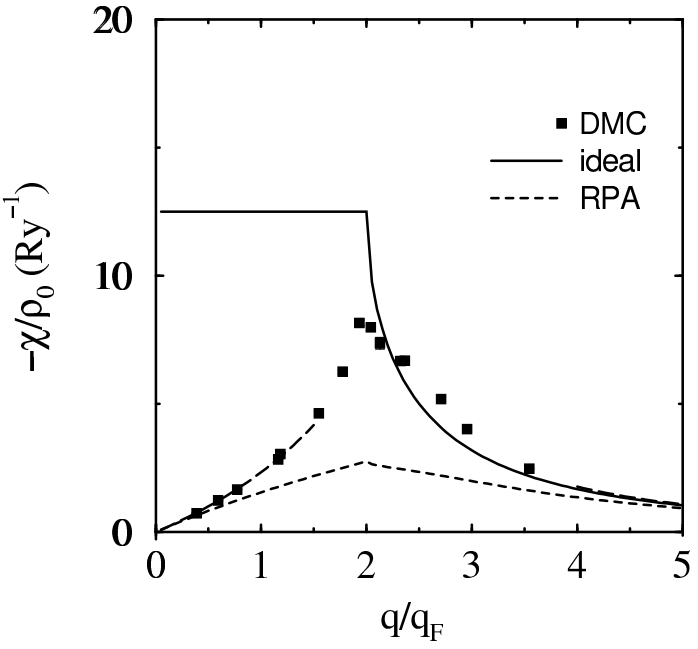

Figure 9. Density–density static response function $\chi(q)$ of the 2d electron gas at $r_s = 5$. The squares give the DMC prediction with error bars. The non–interacting (ideal) and RPA responses are respectively given by the full and the short-dashed curve, whereas the exact[14] small and large q behavior is shown by the long-dashed curves.

with $E_{xc}[\rho]$ the exchange–correlation functional and f_{xc} the exchange–correlation factor. Note that the above equation imposes a constraint on approximate DFT schemes. We shall come back on this point soon. Using Eq. (46) it is easy to show[47] that

$$f_{xc}(q) \longrightarrow \frac{d\mu_{xc}}{d\rho_0}, \quad q \longrightarrow 0, \tag{47}$$

with μ_{xc} the exchange–correlation chemical potential of the electron gas. Evidently, the equation above fixes the small q behavior of $G(q)$. With different techniques it is also possible to determine the leading behavior of $G(q)$ at large q[48, 14, 16].

2.2.2. *Density-density response of the 2d electron gas*

As we mentioned above, all our DMC simulations for Fermions have been performed within the fixed–node approximation. We have calculated the static linear response of the 2d electron gas at three values of the density

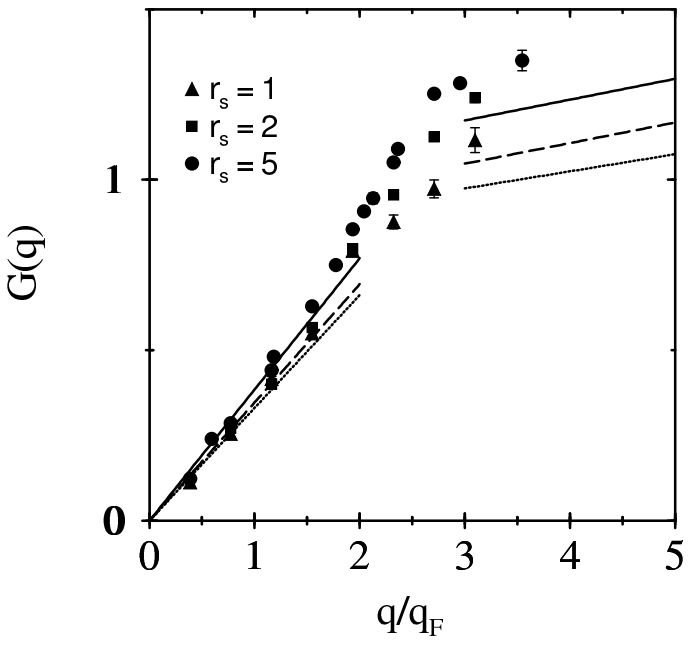

Figure 10. Local field function $G(q)$ of the 2d electron gas. The various symbols (with error bars) give the DMC results at various couplings, as shown. The exact small and large q leading behavior is shown by the short-dashes, long-dashes, and full curve, in order of increasing r_s.

parameter $r_s = 1, 2, 5$, typical of experimental situations. We remind the reader that the parameter r_s, which is defined in the caption to Fig. 1, also gives a measure of the coupling strength in the system, as the ratio of the typical potential to kinetic energy. Thus, small r_s means high density and small coupling, and vice versa for large r_s.

In Fig. 8 we show the density–density response of the 2d electron gas at $r_s = 1$. Already at this small coupling effects beyond RPA are large, as shown by the sizeable difference between the mean field and DMC predictions. Such discrepancies increase with the coupling, as is clear from Fig. 9, where we show results for the system with the largest coupling that we have studied to date, $r_s = 5$. In fact, to isolate the effects beyond RPA one should look at $G(q)$. Thus in Fig. 10 we collect all our local field data. Evidently the local field is appreciable at all couplings and does not change too much in going from $r_s = 1$ to $r_s = 5$. $G(q)$ appears to follow its exact small q behavior at least up to q_F, if not further. On the other hand, our data do not extend to wavevector large enough for the large q behavior

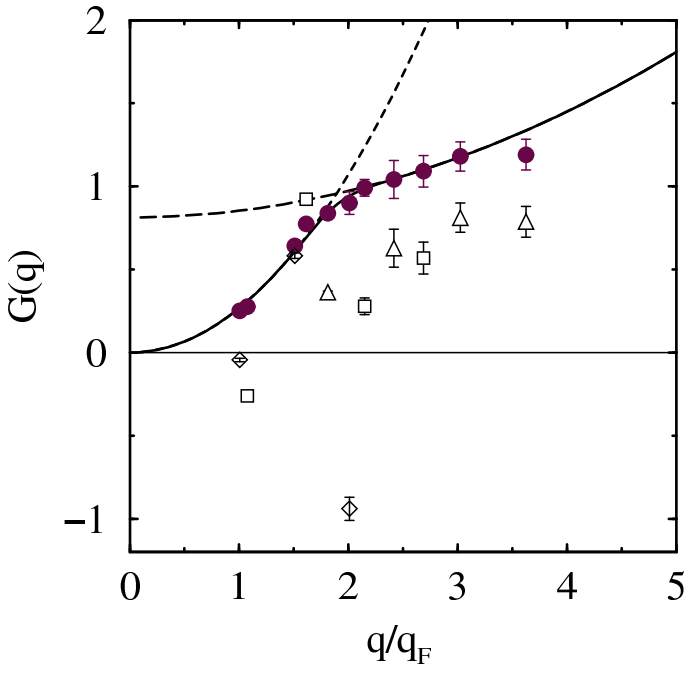

Figure 11. Local field function $G(q)$ of the 3d electron gas at $r_s = 2$. DMC results obtained without size extrapolation are given by the triangles, squares, and diamonds, respectively at $N = 38, 54, 66$. The circles give the same results after applying the size correction of Eqs. (34) and (35). The exact small and large q leading behavior is shown by the short-dashes and long-dashes. Finally, the full curve gives a simple fit[16] to the DMC data. All DMC points are with error bars.

to set it. In this respect, we should emphasize that RPA and full response share the same leading $1/q^2$ term at large q, with their difference being of order $1/q^4$, both in 3 and 2d. Thus at large wavevectors it becomes more and more difficult to extract the local field from the computed response.

2.2.3. *Density-density response of the 3d electron gas*

In 3 dimensions we have computed the linear response of the electron gas[16] at three different densities ρ_0, corresponding to $r_s = 2, 5, 10$, with $4\pi a_0^3 r_s^3/3 = 1/\rho_0$. Some of the observations that we made above for the 2d case remain valid, with obvious differences. Thus, the small and large q behavior of $G(q)$ are quadratic in 3d rather than linear— as implied by Eq. (47) for the small q behavior. Though in terms of $\chi(q)$ (not shown here) the effects of correlation and exchange appear smaller than in 2d—at the same coupling, the local field function shows comparable structure.

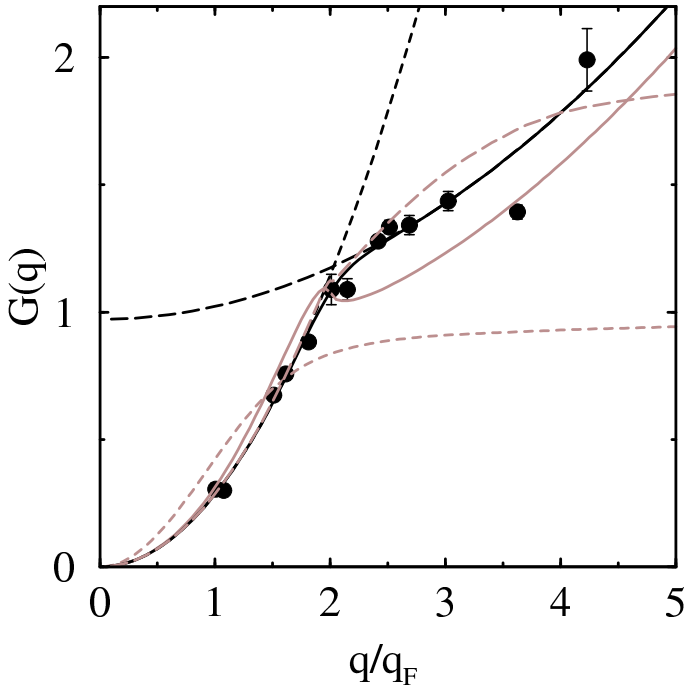

Figure 12. Local field function $G(q)$ of the 3d electron gas at $r_s = 5$. The DMC results are given by the circles (with error bars), whereas exact small and large q leading behavior is shown by the short-dashes and long-dashes. The gray curves give various approximations: the STLS[39] (short dash), Geldart and Taylor[49], and Farid *et al*[50].

In Fig. 11 we display our results for $G(q)$ at $r_s = 2$. We illustrate the importance of size corrections, showing our DMC results both with the correction of Eqs. (34) and (35), and without any correction (i.e., assuming $\chi(\mathbf{q}; N) \approx \chi(q)$). We believe that any comment is superfluous. At this moderate coupling, within the error bars that we have the DMC local field appears to monotonously interpolate between small and large q behavior. The situation somewhat changes when going to larger coupling. At $r_s = 5$, where we have data at larger values of q (see Fig. 12), the local field develops a minimum around $4q_F$. The presence of a minimum in $G(q)$ at intermediate q is in fact a general feature of Coulomb systems at strong coupling. It is found in the electron gas[51] both in 2 and 3d, and also in the charged Bose fluid[17, 51]. In Fig. 12 we also show the results of few approximations. The older ones, STLS[39] and Geldart and Taylor[49], erroneously go to a constant at large q, with the the second one however which behaves better in the region up to $2q_F$. The approximation of Farid *et al*[50], on the other

hand, though in principle constructed to have the right behavior[48] at large q, clearly fails to recover the correct constant term present in the exact asymptotic limit[48, 16].

2.2.4. *Spin response*
In the formal treatment of response in Secs. 1.1 and 1.3 we focused on an external field coupling to the one–body density and accordingly we got density–density response functions. If one applies to a system of electrons a magnetic field $h(\mathbf{r})$, instead, which couples to the local spin density operator $\hat{m}(\mathbf{r}) = \hat{\rho}_\uparrow(\mathbf{r}) - \hat{\rho}_\downarrow(\mathbf{r})$, $\hat{\rho}_\sigma(\mathbf{r}) = \sum_{i=1}^{N_\sigma} \delta(\mathbf{r} - \mathbf{r}_{i\sigma})$, one obtains spin response functions. The perturbed Hamiltonian in this case is

$$\hat{H}_v = \hat{H}_0 - \int d\mathbf{r}\hat{m}(\mathbf{r})h(\mathbf{r}), \tag{48}$$

which is obtained from Eq. (1) by simply replacing $(\hat{\rho}, v)$ with $(\hat{m}, -h)$. All the magnetic response formalism is obtained from the other equations of Secs. 1.1 and 1.3 by performing the complementary replacement $(\rho, v) \longrightarrow (m, h)$—note the absence of the minus sign in this second substitution, in accord with the conventional definition of magnetic response[1]. Here, we are using reduced units so that $h = -(\mu_B g/2)H$ has the dimensions of an energy, and consequently the magnetic response functions have the same dimensions as the density response functions. In the following we shall denote the linear spin response function with $\chi_s(q)$. Also we shall use spin density and magnetization as synonyms.

For the non–interacting electron gas, with the present definition we have $\chi_s(q) = -\chi_0(q)$. It is well known[39] that for the spin response there is no equivalent of the RPA mean field treatment and to go beyond the ideal results ($\chi_s(q) = -\chi_0(q)$) one has to take into account short–range exchange and correlation effects. Paralleling the density case, one may set

$$\chi_s(q) = -\frac{\chi_0(q)}{1 + v_c(q)G_-(q)\chi_0(q)}. \tag{49}$$

with $G_-(q)$ a new local field function. In fact, in general one defines a *symmetric* function $G_+(q) \equiv G(q)$ and an *antisymmetric* function $G_-(q)$, in terms of spin–spin components[39]

$$G_\pm(q) = \frac{1}{2}\left[G_{\uparrow\uparrow}(q) \pm G_{\uparrow\downarrow}(q)\right]. \tag{50}$$

If one has access to $\chi_s(q)$ the spin local field $G_-(q)$ is immediately obtained as $v_c(q)G_-(q) = -\chi_s^{-1}(q) - \chi_0^{-1}(q)$.

We conclude these brief considerations on magnetic response observing that, similarly to the charge case, the knowledge of of $G_-(q)$ puts constraints on the dependence of the exchange–correlation functional[33, 32]

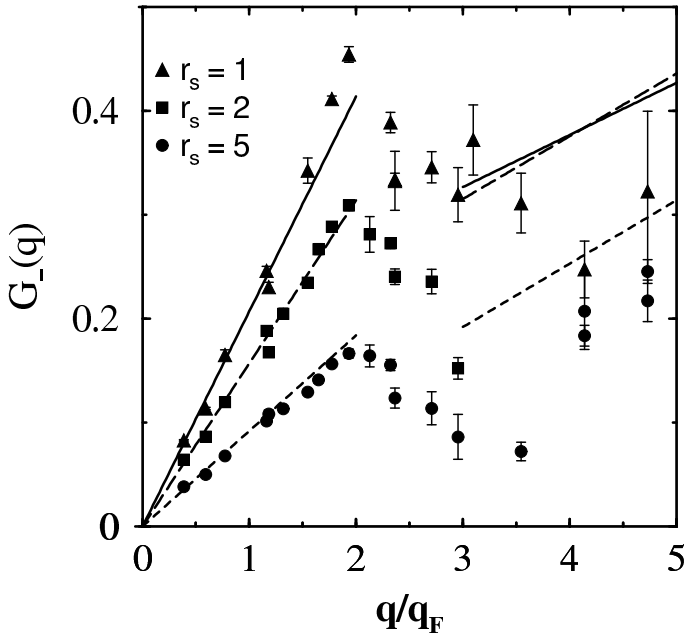

Figure 13. Spin local field function $G_-(q)$ of the 2d electron gas. The various symbols (with error bars) give the DMC results at various couplings, as shown. The exact small and large q leading behavior is shown by the short-dashes, long-dashes, and full curve, in order of decreasing r_s.

on the magnetization density $m(\mathbf{r})$. In particular, for an unpolarized system, if $f_-(q) = -v_c(q)G_-(q)$ one finds

$$f_-(|\mathbf{r}-\mathbf{r}'|) = \left[\frac{\delta^2 E_{xc}[\rho,m]}{\delta m(\mathbf{r})\delta m(\mathbf{r}')}\right]_{\rho_0,m=0}, \tag{51}$$

which yields

$$v_c(q)G_-(q) \longrightarrow -\frac{1}{\rho_0}\left[\frac{d^2\varepsilon_{xc}}{d\zeta^2}\right]_{\zeta=0}, \quad q \longrightarrow 0. \tag{52}$$

Here, ε_{xc} is the exchange–correlation energy per particle of the normal homogeneous fluid, and $\zeta = (\rho_\uparrow - \rho_\downarrow)/(\rho_\uparrow + \rho_\downarrow)$ is the spin polarization.

2.2.5. *Spin–spin response of the 2d electron gas*

We have performed accurate simulations of the spin response in the 2 dimensional unpolarized electron gas[40] at the same couplings for which we

calculated the density response. All the details of the calculations are similar to those for the density case, apart from the fact that the perturbation of Eq. (48) corresponds to opposite one–body potentials acting on opposite spins, and therefore one has different Mathieu orbitals in the two determinants of the trial wavefunction of Eq. (27).

In Fig. 13 we summarize our DMC results for the spin by giving the antisymmetric (spin) local field for the cases that we have studied. It is clear that the spin local field is considerably smaller than the charge one and tends to further decrease at larger coupling. This latter fact is easily understood when one realizes that, at strong coupling, electrons stay well apart in average (the correlation hole becomes more and more pronounced) and differences due to the spin (exchange effects) tend to become smaller.

We have seen above (Eq. (52)) that the small q behavior of $G_-(q)$ is determined by the spin polarization dependence of the exchange–correlation energy. To date this is not know accurately, as there have been no QMC simulations of the 2d electron gas as function of ζ. To estimate $\varepsilon_{xc}(\zeta)$, we extended to 2 dimensions an interpolation ansatz made long ago by Vosko *et al*[52], for the 3d electron gas. The ansatz assumes that $\varepsilon_{xc}(\zeta) - \varepsilon_{xc}(0)$ has the same dependence on ζ as in Hartree–Fock, which yields at once

$$\varepsilon_{xc}(\zeta) = \varepsilon_{xc}(0) + [(\varepsilon_{xc}(1) - \varepsilon_{xc}(0)] \, \frac{(1+\zeta)^{3/2} + (1-\zeta)^{3/2}) - 2}{2^{3/2} - 2}. \qquad (53)$$

Thus, knowing the energies of the unpolarized and of the fully polarized electron gas[53, 54] it is an easy matter to estimate the rhs of Eq. (52). From Fig. 13, one would conclude that the ansatz above is fully compatible with our results for spin response. In fact, blowing up the small q scale or equivalently looking at $\chi_s(q)$, one finds that this is certainly the case at $r_s = 1, 2$, but less obviously so at $r_s = 5$. We close observing that the exact large q behavior of $G_-(q)$ can be obtained (included the constant term) from the known behavior[48, 14, 16] of $G_+(q)$ using the relation $G_+(q) - G_-(q) \longrightarrow 1 - 2g(0), \quad q \longrightarrow \infty$, both in 2 and 3 dimensions.

References

1. See, for instance, D. Forster, *Hydrodynamic fluctuations, broken symmetry, and correlation functions*, Benjamin-Cummings, Reading-Mass (1980).
2. P.C. Martin, in it Many–body physics, edited by C. De Witt and R. Balian, (Gordon and Breach, New York, 1968).
3. In fact, one may consider the case in which several observable are each coupled to a different external field, so that if the unperturbed Hamiltonian is H_0 the total Hamiltonian reads $H = H_0 + \sum_i \int d\mathbf{r} A_i(\mathbf{r}) v_i(\mathbf{r}, t)$. Regardless of having one or several external fields, one may look at the change $\delta\langle A_j(\mathbf{r}, t)\rangle$ in the expectation value of the observable $A_j(\mathbf{r})$ due to the presence of the field $v_i(\mathbf{r}, t)$: to linear order this defines the (cross) linear response function $\chi''_{ij}(\mathbf{r}, \mathbf{r}', t - t')$. The interested reader is urged to check Reference [1] above, especially Sect. 3, for a simple and yet

detailed discussion of the response function formalism. One caution is in order. In Reference [1] a minus sign is used in the coupling, a choice which is natural when dealing with magnetic response: this implies an extra minus sign in the definition of the linear response functions and in many ensuing relations, as compared with the present treatment.

4. H.B. Callen and T.A. Welton, Phys. Rev. B **83**, 34 (1951).
5. From QMC simulations one can easily obtain for Bosons the intermediate scattering function in imaginary time $F(\mathbf{q},-i\tau)$, with acceptable accuracy. $F(\mathbf{q},-i\tau)$ is the analytic continuation of the real time function obtained taking the inverse transform of Eq. (13). At $T=0$, in particular, one gets $F(q,-i\tau)=\int_0^\infty d\omega S(q,\omega)e^{-\omega\tau}/2\pi$ and from this $-(2\rho/\hbar)\int_0^\infty d\tau F(q,-i\tau)=-(\rho/\pi\hbar)\int_0^\infty d\omega(S(q,\omega)/\omega)=\chi(q)$.
6. M. Boninsegni and D.M ceperley, J. Low Temp. Phys. **104**, 339 (1996).
7. Stefano Baroni and Saverio Moroni, *Reptation Quantum Monte Carlo*, this book. See, in particular Sec. 5.2.
8. We caution the reader that in the literature on Helium often slightly different definitions are used. In linking $F(q,t)$ and $S(q,\omega)$ the rhs of Eq. (13) is divided by 2π. Moreover the response function $\chi(q)$ is defined to include a factor $1/\rho_0$, so as to have dimensions 1/energy, rather than 1/(energy×volume) as in the present paper.
9. D.M Ceperley and M.H. Kalos in *Monte Carlo Methods in Statistical Physics*, edited by K. Binder, (Springer–Verlag, Berlin, 1979).
10. P.J. Reynolds, D.M. Ceperley, B. J. Alder, and W.A. Lester, J. Chem. Phys. **77**, 5593 (1982);
11. D.M. Ceperley, *Lectures on Quantum Monte Carlo*, in *Computational Physics*, ICTP,Trieste (1997); a postscript version of these notes can be downloaded from *http://www.ncsa.uiuc.edu/Apps/CMP/papers/cep96b/*.
12. S. Moroni, D.M. Ceperley, and G.Senatore, Phys. Rev. Lett. **69**, 1837 (1992).
13. G. Sugiyama, C. Bowen, and B. J. Alder, Phys. Rev. B **46**, 13042 (1992).
14. S. Moroni, D.M Ceperley and G. Senatore, in *Strongly Coupled Plasma Physics*, edited by by S. Ichimaru and H.M. Van Horn, (University of Rochester Press, Rochester, 1993).
15. C. Bowen, G. Sugiyama, and B.J. Alder, Phys. Rev. B **50**, 14838 (1994).
16. S. Moroni, D.M. Ceperley, and G. Senatore, Phys. Rev. Lett. **75**, 689 (1995).
17. S. Moroni, S. Conti, and M. P. Tosi, Phys. Rev. B **53**, 9688 (1996).
18. G. Senatore, S. Moroni, D.M. Ceperley, J. Noncryst. Solids **205-207** 851 (1996).
19. G. Senatore, S. Moroni, D.M. Ceperley, in *Physics of Strongly coupled plasmas*, edited by W.D Kraeft and M Schlanges (World Scientific, Singapore, 1996).
20. see, also, C. J. Umrigar, M. P. Nightingale, and K. J. Runge, J. Chem. Phys. **99**, 2865 (1993).
21. L. Mitas, *Diffusion Monte Carlo*, this book.
22. Such an error can be avoided for ground state averages of R–space diagonal operators that do not commute with the hamiltonian by resorting to the forward walking technique[55, 56, 57]. However, for the sake of simplicity we chose not to implement this method in our simulations, as we already had an unbiased route to response functions.
23. We note that use of the energy route to the the density–density response requires in general calculations for both the unperturbed and the perturbed system. In fact, one may perform calculations only for the perturbed system and regard ε_0 as an additional fitting parameter. In general we chose to calculate ε_0 from a direct simulation of the unperturbed system, on the ground that this procedure should be more precise, being independent of the details of the fitting. Also, the explicit calculation of the unperturbed system provides us with an additional check on the fact that the perturbed system indeed approaches the unperturbed one as v approaches 0.
24. M. H. Kalos, M. A. Lee and P. A. Whitlock, and G. V. Chester, Phys. Rev. **B24**, 115 (1981).

25. See, e.g., S. Moroni, S. Fantoni, and G. Senatore, Europhys. Lett. **30**, 93 (1995); Phys. Rev. **B 52**, 13547 (1995).
26. D. M. Ceperley, Phys. Rev. B **18**, 3126 (1978).
27. D.M. Ceperley and B.J. Alder, Phys. Rev. Lett. **45**, 567 (1980).
28. Y. Kwon, Y., D.M. Ceperley, and R.M. Martin, Phys. Rev. **48**, 6800 (1998).
29. Y. Kwon, Y., D.M. Ceperley, and R.M. Martin, Phys. Rev. **48**, 12037 (1993).
30. Cyrus Umrigar, *Wave function optimization; Metropolis Monte Carlo*, this book.
31. D. M. Ceperley, G. V. Chester, M. H. Kalos, Phys. Rev.**D13**, 3208 (1976).
32. W. Kohn and L. J. Sham, Phys. Rev. **140**, 1133 (1965).
33. P. Hohenberg and W. Kohn, Phys. Rev. **136**, B864 (1964).
34. R. G. Parr and W. Yang, *Density Functional Theory of Atoms and Molecules* (Oxford University Press, New York, 1989).
35. For the charge case one can easily show that, with the notations of Sec. 2.2.4 and working in reciprocal space, $v^{KS}/v_{\mathbf{q}} = [1-v_c(q)[1-G(q)]\chi_0(q)]^{-1}$. On account of the negative sign of χ_0, this yields, for small values of q and in fact whenever $G(q) < 1$, $v^{KS}/v_{\mathbf{q}} < 1$. Simple considerations show in fact that $v^{KS}/v_{\mathbf{q}}$ vanishes with q. Similarly, for a magnetic perturbation one gets $v^{KS}/v_{\mathbf{q}} = 1/[1+v_c(q)G_-(q))\chi_0(q)]$, which yields $v^{KS}/v_{\mathbf{q}} > 1$ whenever $G_-(q) > 0$.
36. Note that with our definition of the external potential strength one has[36] $m_{\mathbf{q}}/\rho_0 = -(1/2)d\varepsilon/dh_{\mathbf{q}}$. Thus the β and γ parameters from the two fits should coincide, in principle. For the charge, from Eqs. (16) and (18)one gets $\rho_{\mathbf{q}}/\rho_0 = (1/2)d\varepsilon/dv_{\mathbf{q}}$, the different sign being just a matter of definition as already mentioned[3]. See, also, Sec. 2.2.4.
37. F. Stern, Phys. Rev. Lett. **18**, 546 (1967).
38. D. Pines and P. Nozières, *Theory of Quantum Liquids* (Benjamin, 1966), Vol. I; P. Nozières and D. Pines, *Theory of Quantum Liquids* (Addison Wesley, 1990), Vol. II.
39. See, for instance, K. S. Singwi and M. P. Tosi, *Solid State Physics*, edited by H. Ehrenreich, F. Seitz and D. Turnbull (Academic, New York, 1981).
40. S. Moroni, D.M. Ceperley, and G. Senatore, in preparation.
41. R.A Cowley and A.D. Woods, Can. J. Phys. **49**, 177 (1971).
42. R. A. Aziz, V. P. S. Nain, J. S. Carley, W. L. Taylor, G. T. Conville, *J. Chem. Phys.* **70**, 4330 (1979).
43. D. Hall and E. Feenberg, Ann. Phys. (N.Y) **63**, 335 (1971).
44. A. Isihara, Solid State Physics **42**, 271 (1991).
45. T. Ando, A. Fowler, and F. Stern, Rev. Mod. Phys. **54**, 437 (1982).
46. See, e.g., N. W. Ashcroft and D. Mermin, *Solid State Physics*, Saunders College (Philadelphia, 1987).
47. See, e.g., S. Moroni and G. Senatore, Phys. Rev. B **44**, 9864 (1991).
48. A. Holas, in *Strongly Coupled Plasma Physics*, ed. F. J. Rogers and H. Dewitt, NATO Advanced Study Institute Series B: (Plenum, New York, 1986), Vol 154.
49. D. J. W. Geldart and Roger Taylor, Can. J. Phys. **48**, 167 (1970).
50. B. Farid, V. Heine, G. E. Engel, and I. J. Robertson, Phys. Rev. B **48**, 11602, (1993).
51. C. N. Likos, S. Moroni, and G. Senatore, Phys. Rev. B **55**, 8867 (1997).
52. S. H. Vosko, L. Wilk, and M. Nusair, Can. J. Phys. **58**, 1200 (1980).
53. F. Rapisarda and G. Senatore, Aust. J. Phys. **49**, 161 (1996).
54. B. Tanatar, and D.M. Ceperley, Phys. Rev. B **39** , 5005 (1989).
55. M.P. Nightingale, *Basics, Quantum Monte Carlo and Statistical Mechanics*, this book. See, in particular Sec. 5.
56. M.H. Kalos, J. Comp. Physics **1**, 257 (1966).
57. K.S. Liu, M.H. Kalos, and G.V.Chester, Phys. Rev. **A10**, 303, (1974).